Generation of Space-Charge Waves due to Localized Perturbations*

J. G. Wang, D. X. Wang, D. Kehne, and M. Reiser
Laboratory for Plasma Research and Department of Electrical Engineering
University of Maryland, College Park, Maryland 20742

Abstract

Generation of various space-charge waves due to localized perturbations on the beam parameters, namely the velocity, density, and current, is reported. Analytical solutions of one-dimensional fluid equations under such perturbations are presented and compared with the experimental results.

I. INTRODUCTION

The study of longitudinal instabilities in space-charge dominated beams is an on-going research program at the University of Maryland [1]. It has significant importance to high current beam acceleration and transport such as in the case of induction linacs for heavy ion fusion drivers [2]. As the first phase of the program, we study the generation, propagation, and edge reflection of space-charge waves due to localized perturbations in an environment without instability.

The behavior of space-charge waves has been long studied in the fields of microwave generation and particle acceleration [3,4]. The underlying physics is well known when beams are perturbed by sinusoidal signals. In order to study beam physics of longitudinal instability and beam-wave interaction, it is desirable to generate space-charge waves in the form of localized perturbations instead of sinusoidal signals. There is very little information about this in the literature.

In the experiment we found that the space-charge waves generated by localized perturbations have various forms, depending on how specific beam parameters are perturbed. In general two space-charge waves have different amplitude and polarity under the initial velocity and density perturbations. It is only in some special cases, the two space-charge waves are generated with the same amplitudes. There are also conditions under which the two space-charge waves degenerate into one: a fast wave only or a slow wave only. The experimental results, analytical solutions and a comparison between the two are reported in this paper.

II. EXPERIMENTAL RESULTS

The experimental setup consists of a short pulse electron beam injector [5] and a 5-m long periodic solenoid focusing channel [6]. The electron beam is generated by a gridded electron gun. The initial perturbation is introduced to the beam by modulating the grid pulse with a small bump as shown in Fig. 1. This corresponds to a positive velocity perturbation on the beam particles, which in turn produces the initial density, or current perturbations at different values depending on the gun operation conditions. The various space-charge waves in the form of localized perturbations are then generated and propagate on the beam. The beam current and energy can be measured along the channel for analysis.

* Research Supported by the U.S. Department of Energy.

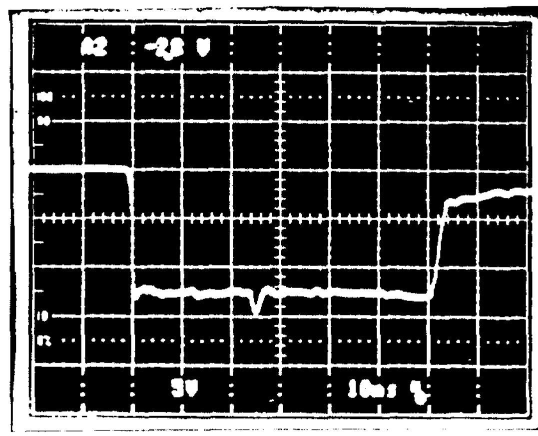

Fig.1. Grid-cathode pulse of the electron gun, showing a perturbation bump.

Figure 2 shows the beam current waveforms measured at 2 different locations along the transport channel. Two current waves, namely, the slow and fast waves appearing in the beam current waveform, are generated in almost equal amplitudes and opposite polarities, and propagate apart.

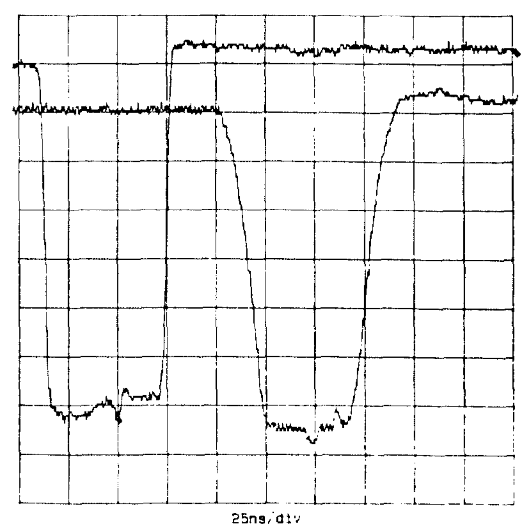

Fig. 2. Beam current waveforms, showing that two current space-charge waves with almost equal amplitudes and opposite polarities propagate away from each other.

Figure 3 shows that only one fast wave with a positive polarity generated on the beam current, which propagates toward the beam front. By contrast, Fig. 4 shows only one slow wave with a negative polarity on the current waveforms, which propagates toward the beam tail.

0-7803-1203-1/93$03.00 © 1993 IEEE

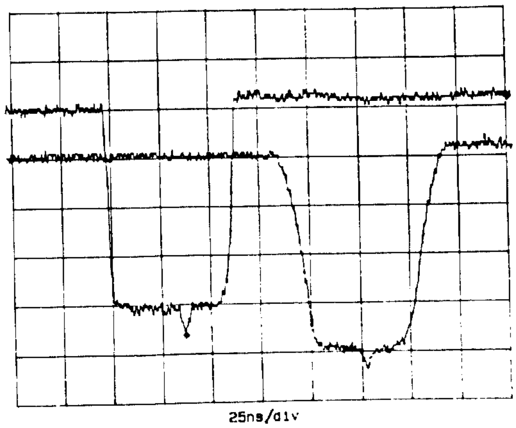

Fig. 3. Beam current waveforms with only one fast wave, propagating towards the beam front.

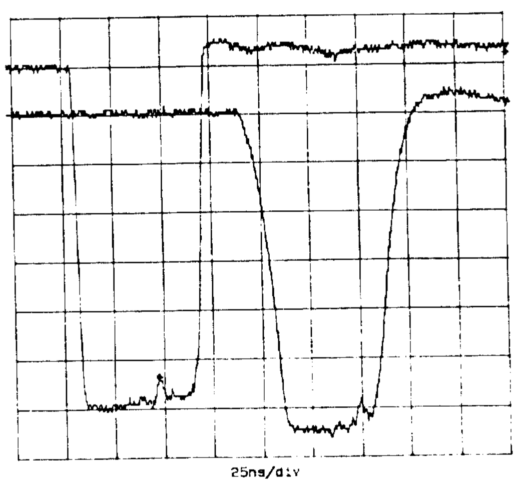

Fig. 4. Beam current waveforms with only one slow wave, propagating towards the beam tail.

Figure 5 shows the space-charge wave signals from an beam energy analyzer, where the beam particles with an energy above the beam average energy pass through the energy analyzer and form the bumps of the traces. On the top trace, only one fast velocity wave appears, corresponding to the case in Fig. 3, while on the bottom trace only one slow wave appears, corresponding the case in Fig. 4. On the fourth trace, two velocity waves with almost the same amplitude appear, that is close to the case in Fig. 2. Other traces show that one velocity wave is dominant over another.

III. ANALYTICAL SOLUTIONS

In order to interpret the experimental observations, the cold fluid model has been employed. The space-charge waves are solved in the time domain for a localized perturbation instead of in the frequency domain for a sinusoidal wave. The specific solutions under the given initial and boundary conditions are obtained instead of eigenmode solutions from dispersion equations. All possible initial conditions of velocity, density, and current perturbations occurred in the experiment are taken into consideration.

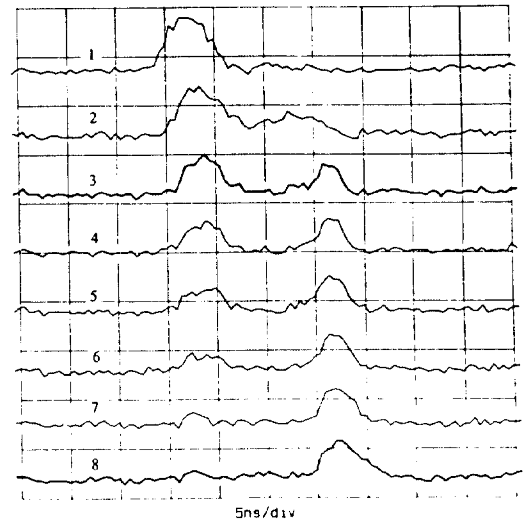

Fig. 5. Velocity waves measured by beam energy analyzer, showing the change from a fast wave to a slow wave when the perturbation conditions vary in the gun.

The one-dimensional fluid model consists of the linearized continuity equation and momentum transfer equation:

$$\begin{cases} \dfrac{\partial\lambda_1}{\partial t} + v_0\dfrac{\partial\lambda_1}{\partial z} + \lambda_0\dfrac{\partial v_1}{\partial z} = 0 \\ \dfrac{\partial v_1}{\partial t} + v_0\dfrac{\partial v_1}{\partial z} \approx \dfrac{e}{m\gamma^3}E_z \approx -\dfrac{eg}{4\pi\varepsilon_0 m\gamma^5}\dfrac{\partial\lambda_1}{\partial z} \end{cases} , \quad (1)$$

where $\lambda(z,t)$ and $v(z,t)$ are the line charge density and the particle velocity, the subscripts 0 and 1 representing the unperturbed and perturbed quantities, respectively, $E_z(z,t)$ is the longitudinal electrical field induced by the a. c. component of the beam current, which equals to $(-g/4\pi\varepsilon_0\gamma^2)(d\lambda_1/dz)$ under the long wavelength condition, g is a geometric factor of order unity, and $e/(m\gamma^3)$ denotes the ratio of the charge and the "longitudinal mass" of the charged particles.

By applying the double Laplace transformations both for the space z and time t, defined by

$$\tilde{f}(k,s) = \int_0^\infty dz \int_0^\infty f(z,t)e^{-(kz+st)}dt \quad , \quad (2)$$

where $f(z,t)$ is a function representing $v_1(z,t)$, $\lambda_1(z,t)$, or $i_1(z,t)$ - the perturbed beam current, Eq. (1) then can be converted to algebra equations for v_1, λ_1 and i_1 in the k-s domain.

Further, we consider the following initial and boundary conditions: a).There is no perturbation anywhere along the z-axis when $t<0$; b). At $z=0$ for $t>0^+$ a local velocity perturbation is introduced to the beam in the form

$$v_1(0,t) = \alpha v_0 G(\tau) \quad , \quad (3)$$

where α is a small quantity to specify the strength of the perturbation, and $G(\tau)$ is the unit gate function defined by the difference of two Heavyside unit step functions

$$G(\tau) = U(t) - U(t-\tau) \quad ; \quad (4)$$

c). Assume the initial current perturbation has the form

$$i_1(0, t) = \beta i_0 G(\tau) \quad , \tag{5}$$

with β as a small quantity to specify the perturbation strength. Therefore, the initial density perturbation is determined by

$$\lambda_1(0, t) = (\beta - \alpha)\lambda_0 G(\tau) \quad . \tag{6}$$

Thus, the perturbed beam parameters can be found as

$$\tilde{\lambda}_1(k, s) = \frac{\beta i_0 s + (\beta - \alpha)\lambda_0\left(v_0^2 - c_s^2\right)k}{\left(s + kv_0\right)^2 - k^2 c_s^2}\frac{1}{s}\left(1 - e^{-s\tau}\right) \quad , \tag{7}$$

$$\tilde{v}_1(k, s) = \frac{\left[\alpha v_0^2 + (\beta - \alpha) c_s^2\right]s + \alpha v_0\left(v_0^2 - c_s^2\right)k}{\left(s + kv_0\right)^2 - k^2 c_s^2}\frac{1}{s}\left(1 - e^{-s\tau}\right) \quad , \tag{8}$$

and

$$\tilde{i}_1(k, s) = v_0\tilde{\lambda}_1(k, s) + \lambda_0\tilde{v}_1(k, s) \quad . \tag{9}$$

Here c_s is the so called "sound" velocity of space-charge waves and defined as

$$c_s = \sqrt{\frac{eg\lambda_0}{4\pi m\varepsilon_0\gamma^5}} \quad . \tag{10}$$

Inverse Laplace transforms yield the perturbed beam density, velocity and current in the real time-space domain as

$$\lambda_1(z, t) = -\frac{\lambda_0}{2}\left[\alpha\frac{v_0}{c_s} - (\beta - \alpha)\right]G_{[z - (v_0 - c_s)t]}(\tau) + \frac{\lambda_0}{2}\left[\alpha\frac{v_0}{c_s} + (\beta - \alpha)\right]G_{[z - (v_0 + c_s)t]}(\tau) \quad , \tag{11}$$

$$v_1(z, t) = +\frac{v_0}{2}\left[\alpha - (\beta - \alpha)\frac{c_s}{v_0}\right]G_{[z - (v_0 - c_s)t]}(\tau) + \frac{v_0}{2}\left[\alpha + (\beta - \alpha)\frac{c_s}{v_0}\right]G_{[z - (v_0 + c_s)t]}(\tau) \quad , \tag{12}$$

$$i_1(z, t) = \frac{-i_0}{2}\left[\frac{\alpha v_0}{c_s} - \beta + \frac{(\beta - \alpha)c_s}{v_0}\right]G_{[z - (v_0 - c_s)\tau]}(\tau) + \frac{i_0}{2}\left[\frac{\alpha v_0}{c_s} + \beta + \frac{(\beta - \alpha)c_s}{v_0}\right]G_{[z - (v_0 + c_s)t]}(\tau) \quad . \tag{13}$$

Here the two-dimensional unit gate function is defined as

$$G_{[z - (v_0 \pm c_s)t]}(\tau) = U\left[z - \left(v_0 \pm c_s\right)(t - \tau)\right] - U\left[z - \left(v_0 \pm c_s\right)t\right] \quad . \tag{14}$$

IV. DISCUSSION

According to Eq. (13), the two current waves have the same amplitudes with the opposite polarity only when $\beta=0$, i.e. without an initial current perturbation. This is the case in Fig. 2. When $\beta/\alpha=(1+v_0/c_s)$, only one fast wave is generated as in the case of Fig. 3. When $\beta/\alpha=(1-v_0/c_s)$, only one slow wave survives as shown in Fig. 4.

Fig. 6 shows the relative amplitude of the velocity waves, i.e. the ratio of the velocity wave amplitude over the initial perturbation amplitude αv_0, versus the quantity β/α for $c_s/v_0=0.1$. It is only at the point A where $\beta/\alpha=1$ indicating the initial density perturbation is zero, the two velocity waves have the same polarity and the same relative amplitude of 1/2. Elsewhere, the two velocity waves have different amplitudes, even different polarity when $|\beta/\alpha|$ is large enough. The sum of the two amplitudes is always 1, i.e. the initial perturbation amplitude, as expected. The slow wave vanishes completely at $\beta/\alpha=11$, while the fast wave vanishes at $\beta/\alpha=-9$. This is compared with the scope traces in Fig. 5.

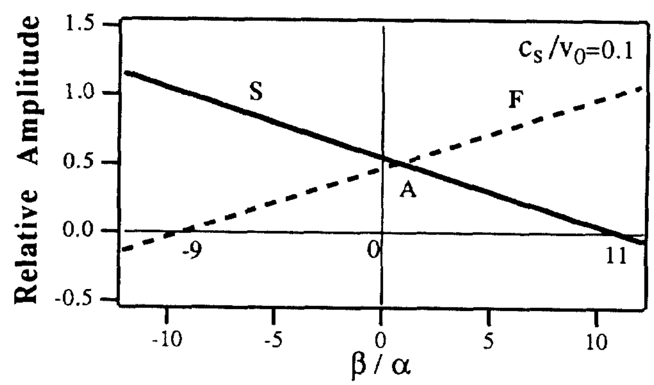

Fig. 6. Relative velocity wave amplitude vs. perturbation parameters.

V. SUMMARY

The generation of space-charge waves due to localized perturbations to the beam parameters is studied experimentally and analytically. Various forms of space -charge waves have been observed and they are the solutions of the fluid model. Good agreement between the theory and experiment has been found.

VI. REFERENCES

[1] J. G. Wang, M. Reiser, W. M. Guo, and D. X. Wang, Particle Accelerators, Vol. **37-38** , 181 (1992).

[2] E. P. Lee, in the Proceedings of the 1992 Linac Conference, Ottawa, Canada, Aug. 24-28, p. 591.

[3] A. H. W. Beck, Space-Charge Waves, Pergamon Press, 1958.

[4] J. D. Lawson, The Physics of Charged Particle Beams, Chapter 6, Oxford University Press, second edition, 1988.

[5] J. G. Wang, D. X. Wang, and M. Reiser, Nucl. Instr. & Meth. in Phys. Res. **A316**, 112 (1992).

[6] D. X. Wang, J. G. Wang, D. Kehne, and M. Reiser, accepted for publication in Applied Physics Letters.